Results in Engineering 26 (2025) 105246

Contents lists available at ScienceDirect

Results in Engineering

journal homepage: www.sciencedirect.com/journal/results-in-engineering

Research paper

Optimal operating conditions of PES/$BiFeO_3$ mixed matrix membrane for treating dye-contaminated wastewater

Shahad K. Jawad [a], Khalid T. Rashid [a,*], Manal Afham Toma [a], Adnan A. Abdul Razak [a], Mohammed Ahmed Shehab [b], Maryam Y. Ghadhban [a], Munaf Al-lami [c], Alhafadhi Mahmood [d,e,*], Haidar Hasan Mohammed [c,f], Amaal Ajeel Hmood [g], Mohammed Faleh Abd Al-Ogaili [h], Saad Alsarayefi [i]

[a] Membrane Technology Research Unit, Chemical Engineering Department, University of Technology- Iraq, Alsinaa Street 52, 10066 Baghdad, Iraq
[b] Polymers and Petrochemicals Engineering Department, Basrah University for Oil and Gas, 61004 Basrah, Iraq
[c] Department of Chemical Engineering and Petroleum Refining, Basrah University for Oil and Gas, Basrah 61004, Iraq
[d] Department of Mechanical and Energetic, University of Dunaújváros, Dunaújváros, Hungary
[e] Department of Mechanical Engineering, University of Sumer, Rifai, Iraq
[f] Thermodynamics and Mathematical Physics Unit, Faculty of Engineering, University of Mons, 7000 Mons, Belgium
[g] Civil Engineering Department, College of Engineering, Al-Nahrain University, Baghdad, Iraq
[h] Department of Aeronautical Engineering Technologies, Alfarahidi University, Baghdad, Iraq
[i] Petroleum & Gas Engineering Department, University of Thi-Qar, Nasiriyah 64001, Iraq

ARTICLE INFO

Keywords:
Bismuth ferrite
PES/$BiFeO_3$ membrane
Response surface methodology
Optimization

ABSTRACT

In order to manufacture mixed matrix membranes (MMMs) for the treatment of dye-contaminated wastewater, this work intends to optimize the operational and manufacturing factors influencing the incorporation of (Bismuth Ferrite) nanoparticles ($BiFeO_3$ NPs) into Poly(ether-Sulfone) (PES/$BiFeO_3$). A regression model for the investigation of permeate flux and percentage removal was developed using response surface methods (RSM) and analysis of variance (ANOVA). A set of experimental runs for the ultrafiltration (UF) setup was constructed utilizing the central composite design of experiment method. This study examined how operating and preparation conditions affected PES/$BiFeO_3$ membrane permeate flux and MB rejection for all membrane samples. $BiFeO_3$ NPs content (0–0.4 wt.%), MB dye concentration (5–12.5 ppm), and transmembrane pressure (1 to 4) bar were among the variables examined. The operational parameters were further optimized for the intended removal conditions using the developed models. For maximal permeate flux (63.5 LMH) and 97.974 % Congo red dye removal, the optimum operating and preparation parameters were determined to be 0.25, 10 ppm, and 2.57 bar for $BiFeO_3$ concentration, initial dye concentration, and operation pressure, respectively. After being tested under experimental conditions, the developed model was determined to be the best fit. The PES/$BiFeO_3$ membranes shown improved flux and separation capabilities, according to the optimization findings, which makes them appropriate for treating hazardous dye wastewater in a variety of applications.

1. Introduction

Water is an essential element of life, and the lack of clean water is a problem. Water is one of the most critical natural resources. Because of the ongoing development of industrial activities, on the other hand, the wastewater is polluted by different chemicals with increasing production volume, which affects the lives of all living beings [1]. It is essential to provide fresh water for all humans developing industrial and urbane activities and treat the produced wastewater pollution to overcome the problems of water scarcity and pollution, population growth, and increased demand for water due to various industrialization [2,3]. These elements inspired scientists to develop contemporary, sophisticated, sustainable, and clean technology to treat wastewater and provide fresh water, thereby addressing the above listed issues. Due to a vastly large number of industrial pollutants that are discharged into sewage in various industrial sectors, particularly, the discharged dyes and

* Corresponding authors.
E-mail addresses: Khalid.t.rashid@uotechnology.edu.iq (K.T. Rashid), Alhafadhi@uniduna.hu (A. Mahmood).

https://doi.org/10.1016/j.rineng.2025.105246
Received 21 March 2025; Received in revised form 28 April 2025; Accepted 7 May 2025
Available online 8 May 2025

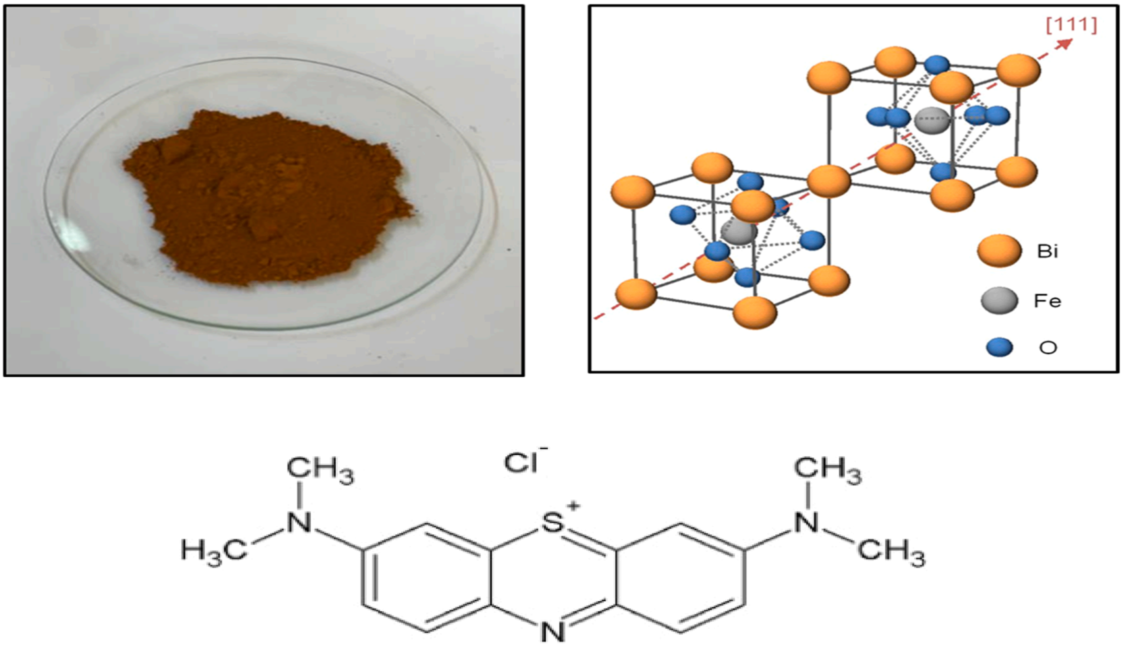

Fig. 1. Bismuth Ferrite ($BiFeO_3$).

Table 1
Membranes composition.

Sample	PES (wt.%)	$BiFeO_3$ (wt.%)	DMF (wt.%)
SM0	20	0	80
SM1	20	0.1	79.9
SM2	20	0.2	79.8
SM3	20	0.3	79.7
SM4	20	0.4	79.6

Table 2
Code and levels of factors.

Variables	Coded	Unite	Low level	High level
Add. Conc.	A	wt.%	0	0.4
Dye Conc.	B	ppm	5	12.5
Press.	C	bar	1	4

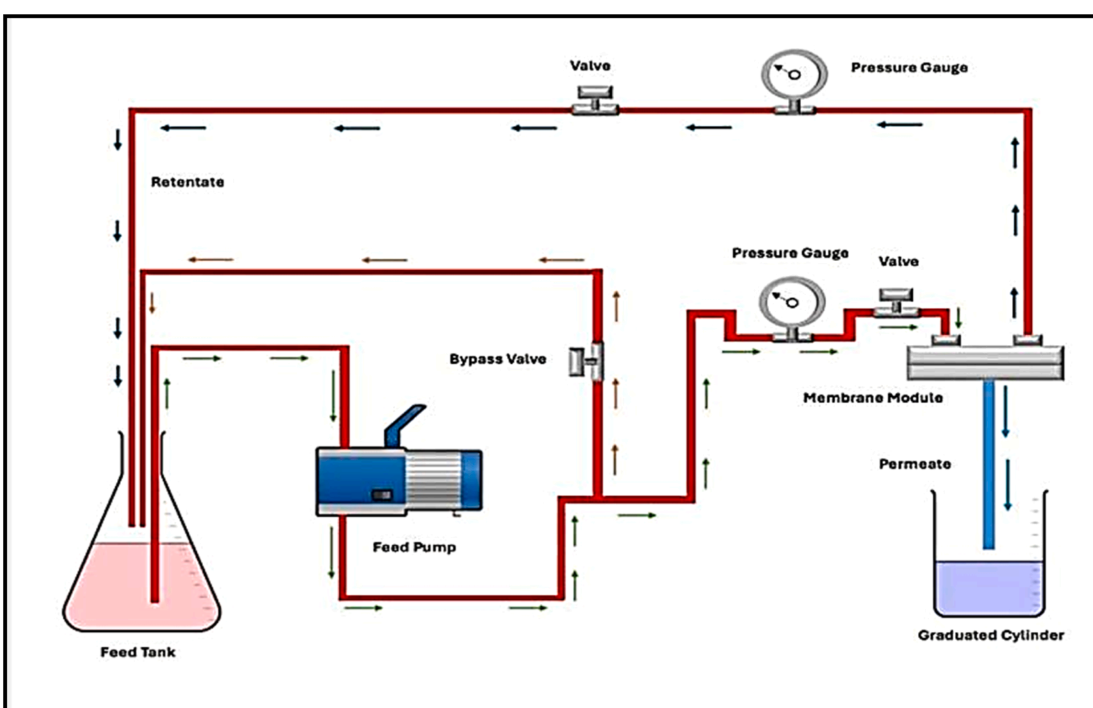

Scheme 1. Schematic diagram of the UF cross-flow filtration system.

Table 3
Experimental data points and response.

Run	Add Con.	Feed Con.	Press	Exp. Flux (LMH)	Pred. Flux (LMH)	Flux Abso. Error %	Exp. Rejection (%)	Pred. Rejection (%)	Rejection Abso. Error %
1	0.30	5.00	1.00	39.7	40.93	3.11	99	99.78	0.79
2	0.30	5.00	4.00	63.5	64.46	1.51	95.5	95.82	0.32
3	0.30	5.00	3.00	60.3	59.57	1.21	97.1	96.73	0.38
4	0.30	5.00	3.00	60.3	59.57	1.21	97.1	96.73	0.38
5	0.30	5.00	3.00	60.3	59.57	1.21	97.1	96.73	0.38
6	0.30	12.50	3.00	58.4	59.85	2.48	99	100.39	1.40
7	0.30	5.00	3.00	60.3	59.57	1.21	97.1	96.73	0.38
8	0.00	10.00	4.00	18.1	17.68	2.33	76.2	76.18	0.02
9	0.40	12.50	4.00	38.2	36.36	4.81	99	97.38	1.64
10	0.30	5.00	3.00	60.3	59.57	1.21	97.1	96.73	0.38
11	0.00	10.00	1.00	9.7	8.82	9.04	85.4	85.14	0.31
12	0.30	5.00	3.00	60.3	59.57	1.21	97.1	96.73	0.38
13	0.30	10.00	3.00	58.4	54.14	7.29	98	97.77	0.3
14	0.40	12.50	1.00	17.2	17.27	0.40	96.1	96.44	0.35
15	0.40	10.00	4.00	34.3	35.65	3.92	93.2	94.67	1.57
16	0.40	10.00	1.00	14.9	14.10	5.44	95.5	94.61	0.93
17	0.40	5.00	3.00	28.8	30.10	4.53	93.1	93.80	0.76
18	0.00	12.50	4.00	15.2	15.07	0.89	80.1	79.96	0.17
19	0.00	12.50	1.00	8.2	8.62	5.18	88	88.02	0.03
20	0.00	5.00	3.00	22.4	23.29	3.97	75.8	76.19	0.52
Mean absolute error %						3.11			0.57
Predication accuracy %						96.89			99.43

Table 4
Analysis of variance (ANOVA) of membrane permeate flux.

Source	Sum of Squares	df	Mean Square	F Value	p-value Prob > *F*	
Model	8322.61	9	924.73	517.33	< 0.0001	significant
A-A	90.55	1	90.55	50.66	< 0.0001	
B-B	3.13	1	3.13	1.75	0.2151	
C-C	418.65	1	418.65	234.21	< 0.0001	
AB	36.64	1	36.64	20.50	0.0011	
AC	81.49	1	81.49	45.59	< 0.0001	
BC	19.02	1	19.02	10.64	0.0085	
A^2	2307.43	1	2307.43	1290.87	< 0.0001	
B^2	1.16	1	1.16	0.65	0.4387	
C^2	21.60	1	21.60	12.08	0.0060	
Residual	17.88	10	1.79			
Lack of Fit	17.88	5	3.58			
Pure Error	0.000	5	0.000			
Cor Total	8340.49	19				
Std. Dev.	**1.34**		**R-Squared**		**0.9979**	
Mean	**39.44**		**Adj R-Squared**		**0.9959**	
C.V. %	**3.39**		**Pred R-Squared**		**0.9656**	
PRESS	**286.73**		**Adeq Precision**		**59.028**	

Table 5
ANOVA analysis of the rejection.

Source	Sum of Squares	df	Mean Square	F Value	p-value Prob > *F*	
Model	1072.70	9	119.19	119.69	< 0.0001	significant
A-A	310.92	1	310.92	312.22	< 0.0001	
B-B	2.76	1	2.76	2.77	0.1271	
C-C	37.52	1	37.52	37.68	0.0001	
AB	3.56	1	3.56	3.57	0.0880	
AC	41.10	1	41.10	41.27	< 0.0001	
BC	2.32	1	2.32	2.33	0.1580	
A^2	127.71	1	127.71	128.24	< 0.0001	
B^2	6.67	1	6.67	6.70	0.0271	
C^2	0.40	1	0.40	0.40	0.5388	
Residual	9.96	10	1.00			
Lack of Fit	9.96	5	1.99			
Pure Error	0.000	5	0.000			
Cor Total	1082.66	19				
Std. Dev.	**1.00**		**R-Squared**		**0.9906**	
Mean	**92.82**		**Adj R-Squared**		**0.9825**	
C.V. %	**1.08**		**Pred R-Squared**		**0.8928**	
PRESS	**116.05**		**Adeq Precision**		**34.309**	

pigments permeate several sectors of everyday life, such as textiles, paints, cosmetics, pharmaceuticals, food, and printing industries. Consequently, dark wastewater must be treated to eliminate colors alongside other contaminants [4–6]. It is estimated that about 10–15 % of these dyes are released in the form of liquid waste during the dyeing process [7].

Dyes are categorized into three primary classifications: (a) Cationic: all basic dyes, (b) Anionic: directly and reactively acidic and (c) Non-ionic: dispersed dyes [8–10]. Because of their poisonous nature and triggering many major ailments like cancer, skin disorders, and allergies, dyes and their metabolic products seriously threaten the environment, particularly living entities [11,12]. The stability of these dyes makes them non-biodegradable, and therefore they exhibit stability in water, and some variants are challenging to treat because of their intricate architecture. Therefore, it is essential to treat and recycle wastewater to save the environment and fulfill certain industrial water needs and/or repurpose dyes [13,14].

Dye removal may be accomplished using a variety of methods, including physical, chemical, and biological processes, which are used in wastewater treatment in order to fulfill the standards that are already in place. One of these procedures is known as an adsorption process [15], deposition by chemical agents [16], and biological means, such as white mold fungus [17], ion exchange [18,19], electrocoagulation [20], and flocculation [21,22] are some of the approaches that have been used. There are some drawbacks associated with these methods, such as the fact that almost all of them do not achieve the required level of dye removal. For instance, biological treatment is an excellent method that is also cost-effective. However, it is not successful in eliminating pollutants that are resistant to heat and microorganisms that may be killed by the toxicity of dyes. The chemical ion exchange process is expensive and can only extract a single compound [23]. Adsorption has garnered significant attention owing to its simplicity, cost-effectiveness, and efficacy in eliminating various dyes from aqueous solutions. Researchers are looking for cost-effective adsorbents with outstanding efficacy in pollution removal. Thus far, to eradicate reactive contaminants from aqueous solutions, various mono and composite adsorbents have been used for this purpose [24], such as GO [25], ZnO [26], MnO_X-CeO_2 [27], $Ag/TiO_2/Fe_3O_4$ [28], MgO/C_3N_4 [29], TiO_2/Fe_2O_3 [30],

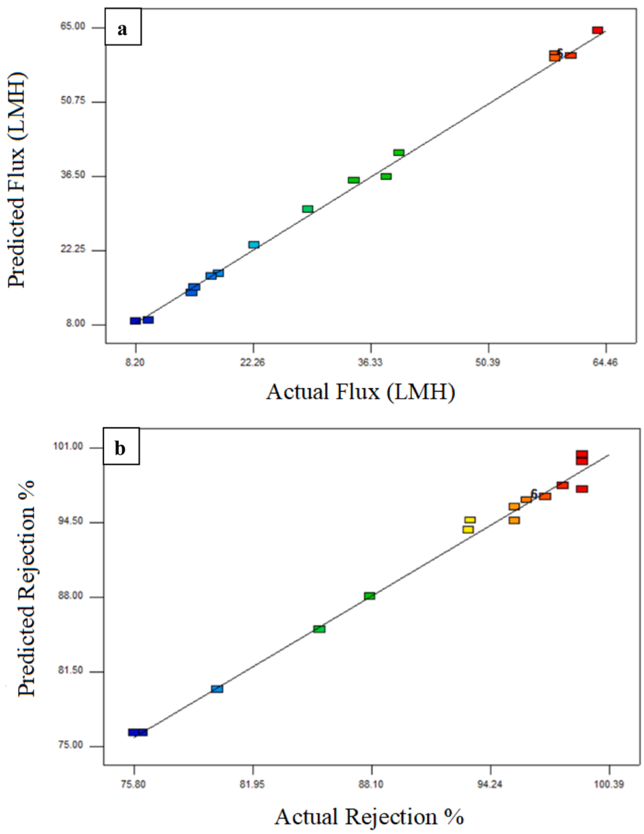

Fig. 2. Predicted and actual results for the (a) membrane flux and (b) rejection %.

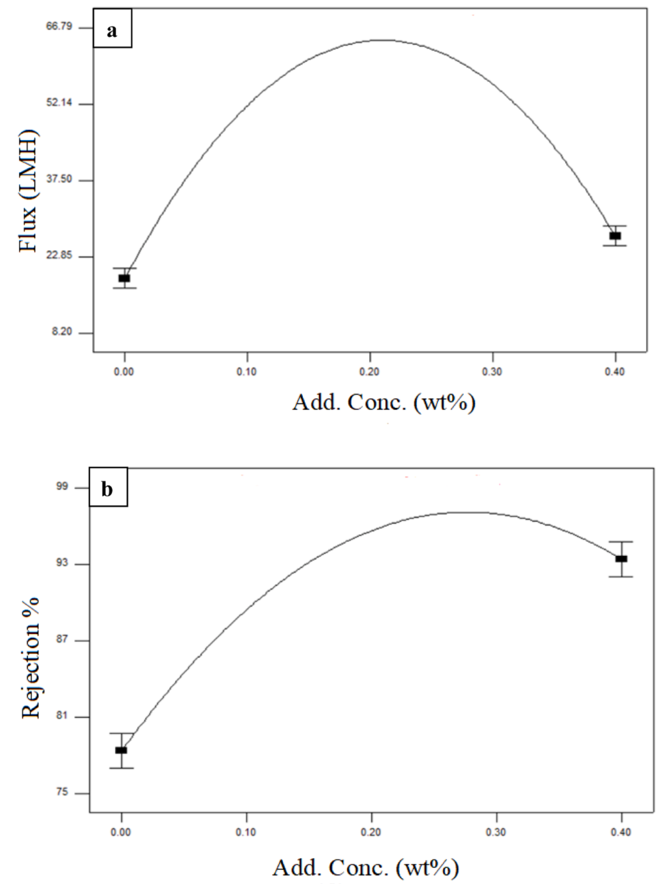

Fig. 3. At constant MB dye concentration 7.5 ppm and pressure 2.5 bar, additives affect a) membrane flux and b) rejection%.

$CdSe/Bi_2MoO_6/g\text{-}C_3N_5$ [31], $Ag/Ag_3VO_4/AgVO_3$ modified with GO [32], chitosan-based MWCNTs/CNCs [33] and CuO/BC [34].

The process performance of adsorption processes is typically influenced by physical and chemical factors, including the reactivity of dye absorbent materials, the surface area of adsorbents, particle size, temperature, pH, contact time, and height maintenance costs, and it decreases after multiple uses. Activated carbon is the most common material used in these processes. Water-soluble dyes are also frequently subjected to flocculation and coagulation [35]. Sometimes, it is challenging to identify the appropriate coagulant to combat the contaminants that result from discoloration [36,37]. Certain procedures necessitate lengthy durations and secondary treatments, while others necessitate a substantial footprint and high energy consumption, resulting in a high cost [38,39].

The effluent of textile industries is challenging to treat due to the presence of complex pigment molecules and their resistance to aerobic digestion, oxidants, light, and heat [40,41]. The advantages and disadvantages of dyes removal have been discussed in nearly all references and studies. In addition to the aggravation of the freshwater crisis and to meet the increasing global demand for its provision, led researchers have to search for advanced new methods and develop new techniques for removing pigments. Among these methods, membrane filtration technology has gained increasing interest over time due to its various advantages [42–46] such as easy to operate, high separation efficiency, no/low need for additional chemicals, reduced energy usage, low running costs, continuous character mode, separation in mild settings, ability to be hybridized with other processes, minimal footprint, and ecologically friendly. Furthermore, membrane filtering technology makes the recovery possibility to remove artificial color from industrial wastewater one of the finest accessible solutions for treating this kind of industrial wastewater [47].

Reverse osmosis (RO), nanofiltration (NF), ultrafiltration (UF), and microfiltration (MF) fall into four varieties [48–50]. UF is an efficient method of ultrafiltration membrane separation for the macromolecule and particle removal from a solution. It has been routinely used as a treatment approach for wastewater discharge from manufacturers including food industry, chemical and pharmaceutical companies [51]. Operating pressure, pore size, separation technique, and membrane feature roughly combine UF membrane with strong rejection, high permeation flow, and low energy usage [52–55]. It has attracted a lot of attention for separating many ions, heavy metals, and dyes [56–58]. Polymers are the most often utilized materials for UF membrane preparation. Sometimes sulfonate-containing polymers, such as polyethersulfone (PES) and polysulfone (PS), are the most used [59–62].

The quality of separation, the expulsion of undesirable particles, the need for less energy, the high mechanical, chemical, thermal, and hydraulic stability of PES-based membranes are among the many advantages [63–67]. In addition, the membrane's hydrophobic nature may result in the surface and apertures being exposed to pollution and obstruction as a result of various foulants. This can result in a reduction in permeability and flow, thereby reducing the membrane's performance efficiency [68–76].

At ambient temperature, bismuth ferrite-$BiFeO_3$ (BFO) (Fig. 1.) is an inorganic, single-phase, type-1 category multiferroic material with both ferroelectric and magnetic characteristics. Because of their characteristics, $BiFeO_3$ nanoparticles were selected for this study. $BiFeO_3$ may be used as photocatalytic materials in addition to its possible magnetoelectric uses. As has been extensively shown in semiconductors, this narrow bandgap also permits carrier excitation in $BiFeO_3$ using commercially accessible femtosecond laser pulses, allowing us to create ferroelectric ultrafast optoelectronic devices. Regarding the photocatalytic activity of BFO, it was shown that $SrTiO_3$ coated BFO

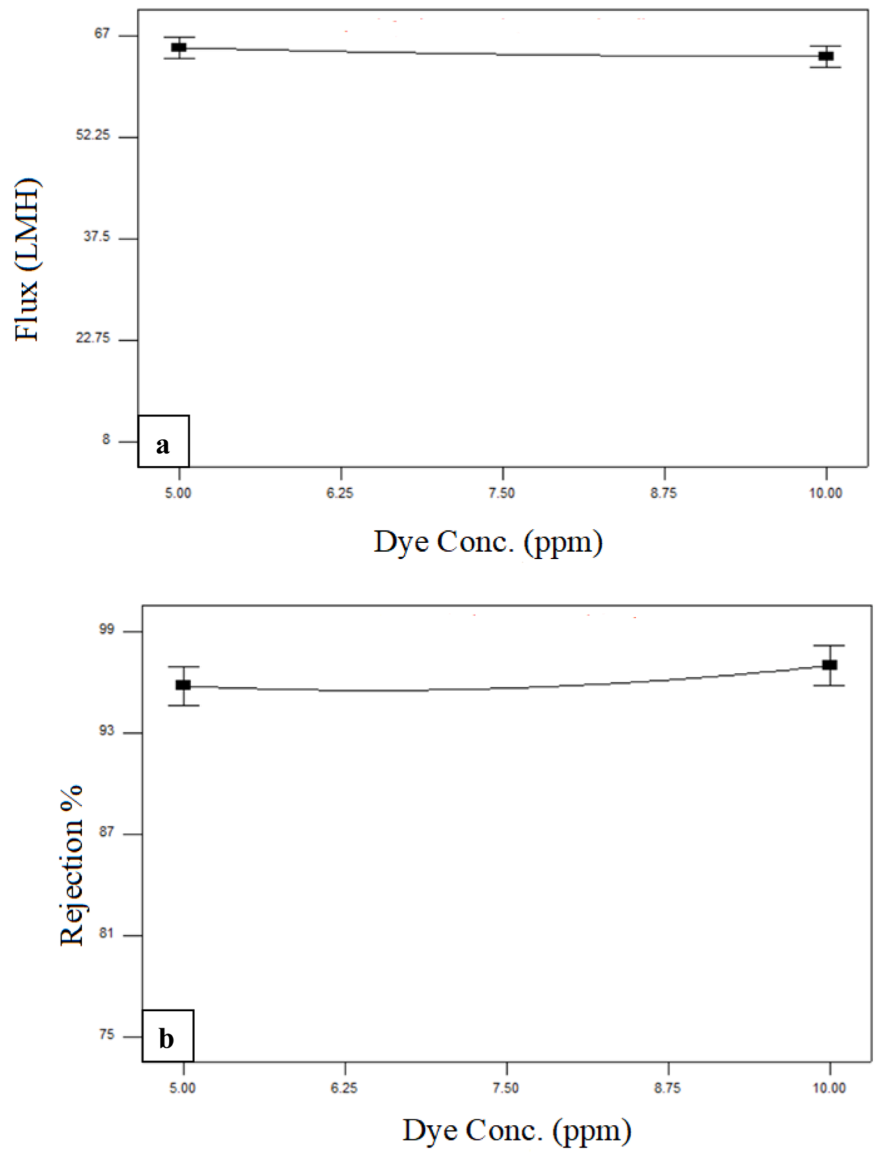

Fig. 4. The influence of MB dye concentration on a) membrane flux and b) rejection percentage with constant pressure of 2 bar and additive concentration of 0.2 wt.%.

nanoparticles may generate H_2 when exposed to visible light, but pure $SrTiO_3$ only reacts to UV irradiation. This is another significant feature. The capacity of $BiFeO_3$ nanowires to oxidize (generate oxygen) was found more recently, indicating that $BiFeO_3$ nanostructures might be helpful for the photocatalytic breakdown of organic pollutants [77–79].

Probably the only substance that is both magnetic and strong ferroelectric at normal temperature is $BiFeO_3$. With hundreds of papers published in the last several years, it has therefore had an influence on the area of multiferroics equivalent to that of yttrium barium copper oxide (YBCO) on superconductors [80]. Few authors have designed trials to optimize the UF membrane for process factors in dye-contaminated wastewater treatment. The combination of simultaneous optimization and non-linear regression analysis for response prediction has not been investigated previously. In order to optimize process variables for the elimination of MB dye in the UF membrane filtration process, in this study, the central composite design (response surface technique) was used. Response surface methodology (RSM) and variance analysis (ANOVA) were used in the study. Herein, the study focused on optimizing different operating parameters such as $BiFeO_3$—NPs content (0–0.4 wt.%), MB dye concentration (5–12 ppm), and transmembrane pressure (1–4 bar), using Design-Expert® software. The purpose of these tests was to ascertain how they affected the MB dye rejection percentage and membrane flux. The study also looked into how operating parameters work together to maximize the performance of PES/$BiFeO_3$-based membranes.

2. Materials and methods

2.1. Materials

The base polymer for membrane manufacture was polyethersulfone (PES) with a molecular weight of 30,000 g/mol, which was obtained from Solvay Advanced Polymers in Belgium, methylene blue (MW = 319.85 g/mol), Di-methyl-formamide (DMF) solvent were obtained from HIMEDIA India Company. Congo red dye Congo red dye (Mw = 696.66 g/mol, excitation wavelength is 497 nm.) used for membrane rejection test were purchased from Nanjing Duly Biotech Co., China. Iron nitrate nonahydrate ($Fe(NO_3)_3{\cdot}9H_2O$) was purchased from CARLO ERBA Reagents, France, Bismuth (III) nitrate pentahydrate ($Bi(NO_3)_3{\cdot}5H_2O$) was purchased from thermos scientific, Hungary,

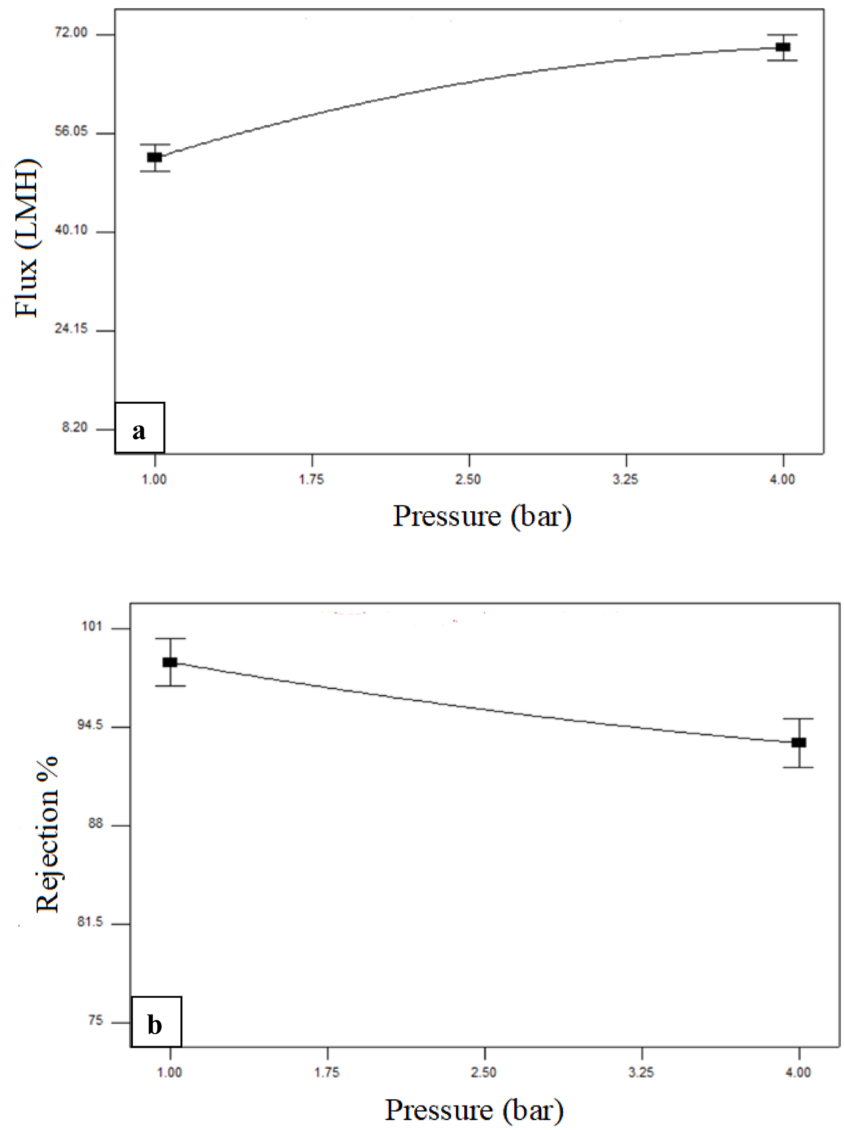

Fig. 5. For membranes at constant MB dye conc. 7.5 ppm and $BiFeO_3$ conc. 0.2 wt.%, operation pressure influence on a) flow and b) rejection% is investigated.

Absolute Ethanol (EtOH) was ordered from VWR International Ltd., Hungary and Ethylene glycol (EG) was obtained from Sigma-Aldrich (Switzerland). Bismuth Ferrite ($BiFeO_3$) was used as an additive loaded in the polymer casting solution.

2.2. Preparation of $BiFeO_3$ nano additives

Bismuth ferrite ($BiFeO_3$) nanoparticles were prepared using the hydrothermal method as described in [81]. Briefly, 0.7 g of Bi $(NO_3)_3{\cdot}5H_2O$ dissolved in 50 mL of an EtOH and EG mixture solution with (1:9) ratios, respectively. Then 0.58 of Fe $(NO_3)_3{\cdot}9H_2O$ was added to the solution and stirred for 30 min. The solution transferred to a stainless-steel Teflon autoclave and thermally treated for 24 h at 180 C. After that, the solid product obtained washed several times with distilled water using vacuum filtration and dried at 75 °C overnight. Finally, the powder form product calcinated for 2 h at 500 °C.

It is possible to postulate the following for the NP formation kinetics in HE processes as:

$$Bi(NO_3)3 \rightarrow Bi^{+3} + 3NO_3{}^{-} \quad (1)$$

$$Fe(NO_3)3 \rightarrow Fe^{+3} + 3NO_3{}^{-} \quad (2)$$

$$Bi^{+3} \rightarrow 3OH^{-} + Bi(OH)_3 \quad (3)$$

$$Fe^{+3} \rightarrow 3OH^{-} + Fe(OH)_3 \quad (4)$$

$$2Bi(OH)3 \rightarrow Bi^{+3} + 3H2O \quad (5)$$

$$2Fe(OH)3 \rightarrow FeO_3 + 3H2O \quad (6)$$

$$Bi_2O_3 \rightarrow Fe_2O_3 + 2BiFe_3 \quad (7)$$

2.3. Preparation of UF membranes

Phase inversion method utilized to produce all the flat sheet UF membranes. The PES polymer powder was oven-dried at 50 °C overnight to eliminate moisture before the casting solution was prepared. Towards the pristine preparation of PES membranes, then, the solvent Di-methyl-formamide (DMF) was used to create the solution in a glass beaker at ambient temperature. Separately included were $BiFeO_3$ NPs at 0, 0.1, 0.2, 0.3, and 0.4 wt percent. and agitated the solution for two hours with a magnet stirrer until homogenized. Adding 20 wt. % of PES polymer and the stirring process continues for 8 h to obtain a suitable dispersion. The solution was subjected to an ultrasonic immersion for a duration of

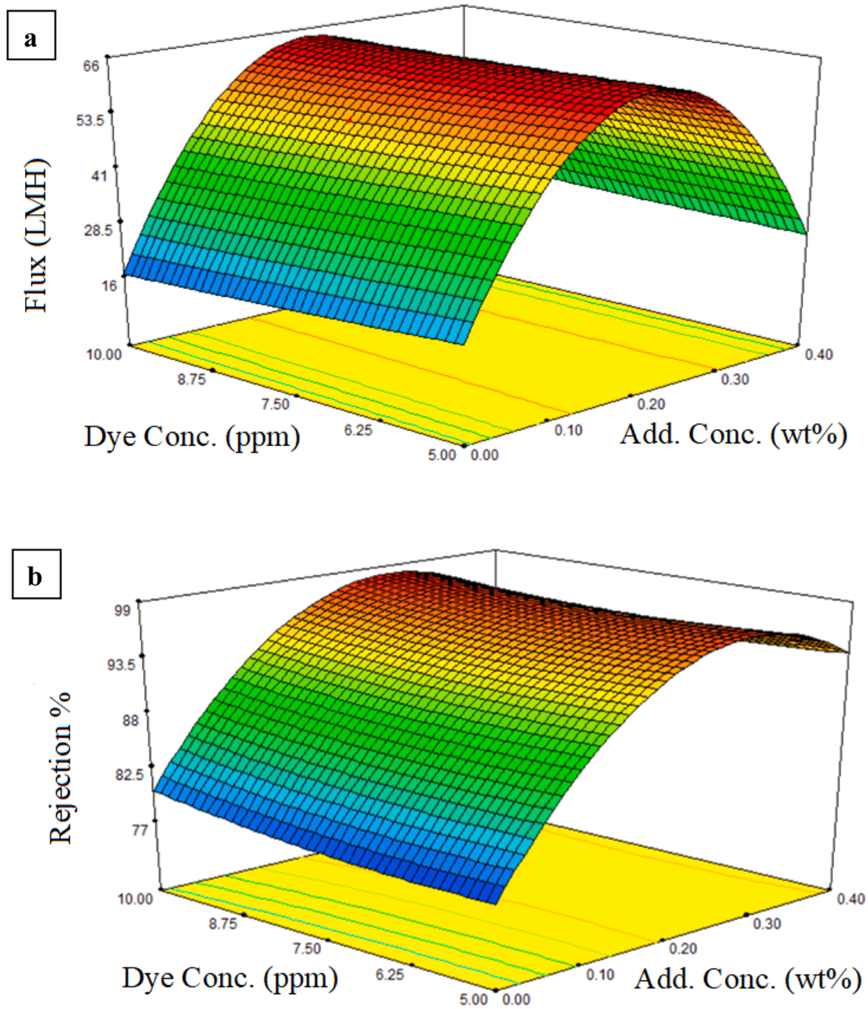

Fig. 6. Effect of dye concentration and additive concentration on a) flux and b) rejection (%) at pressure 2.5 bar.

30 min. Prior to commencing the casting procedure, the solution was pre-treated in an oven preheated to 40 °C for an hour in order to eliminate any residual bubbles. Then, using the casting machine with a 200 nm air gap casting knife, the homogenous solution is poured onto a flat glass. The flat glass is submerged in a room temperature bath of distilled water once the pouring is stopped, and the knife is dragged over it. Casting solution composition of different membranes are given in Table 1.

3. Membrane performance

A cross-flow filtering system Scheme 1. with an effective area of 16 cm^2 was used to evaluate the membrane performance at room temperature. The analysis of membrane penetration was conducted using a pure water flux (PWF) and solutions of 50, 100, and 200 ppm MB. The permeate flow (J) was determined using Eq. (8) [82–84]:

$$J = \frac{Q}{A \times t} \tag{8}$$

where Q is the permeate collected (m^3) with the (t) time, and the effective membrane area (m^2) is A in the filtration cell. The rejection of the MB dye solution was calculated utilizing Eq. (9) [85]

$$R(\%) = \left(1 - \frac{C_p}{C_f}\right) x100 \tag{9}$$

4. Experimental design

A set of tests can be created using a statistical and mathematical approach through response surface methodology (RSM). The Central Composite Design (CCD) of Response Surface Methodology (RSM) was applied, not the Box-Behnken Design. CCD was selected due to its ability to efficiently fit a second order (quadratic) model and explore both linear and interaction effects of the variables across a wide range. Unlike the Box-Behnken Design, CCD includes axial points, allowing for a more thorough investigation of factor extremes. This made it particularly suitable for studying and optimizing the effects of MB dye concentration, transmembrane pressure, and $BiFeO_3$ concentration on membrane performance. The goal is to improve the reaction, which is affected by several separate elements. A further benefit of using the RSM design is that it requires less trials than a full experimental design at the same level. Additionally, the ultimate objective of RSM is to determine the area that satisfies the operational parameters or the ideal operating circumstances for the system. RSM drastically lowers time and material costs as compared to the "one factor at a time" method [86].

Design-Expert® Software was used to perform the analyses. To evaluate their effects on the flux and rejection percentage of the membranes, the current study concentrated on optimizing various operational parameters, including the concentration of MB dye (5 to 12.5 ppm), the transmembrane pressure (1 to 4 bar), and the $BiFeO_3$ concentration (0 to 0.4 wt. %). Additionally, the research looked at how operational variables collaborated to affect the result. ANOVA is a

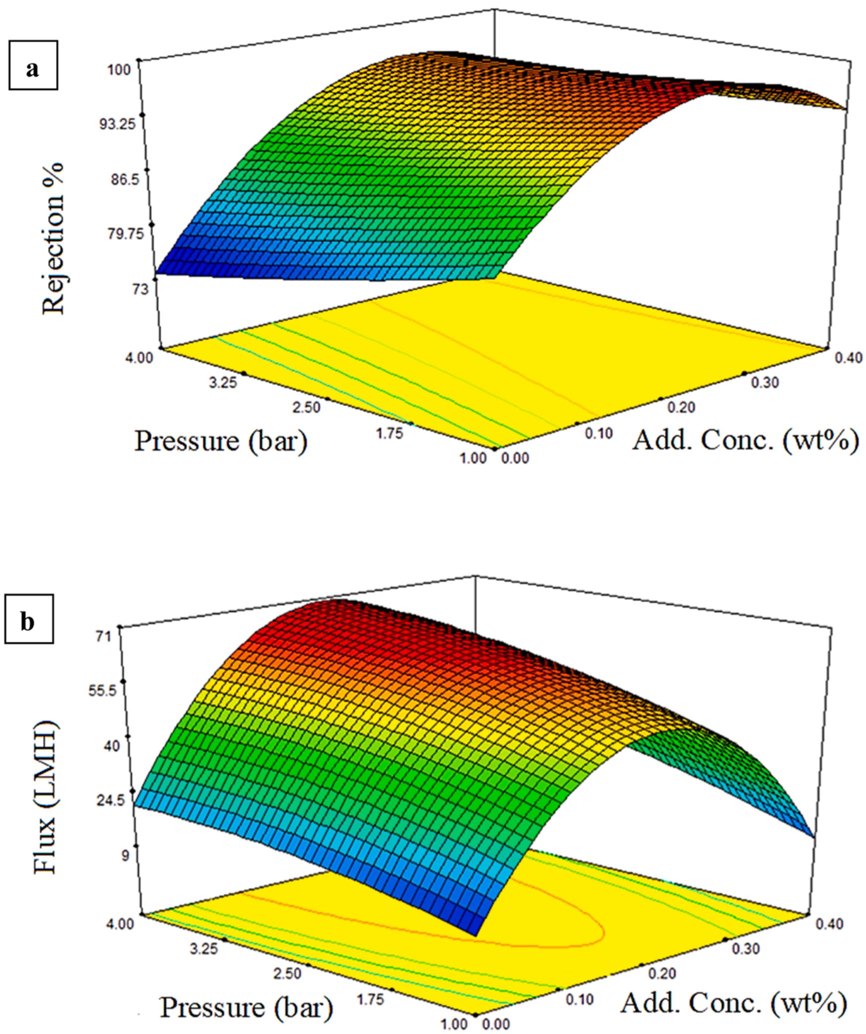

Fig. 7. Behavior of a) permeate flux and b) rejection (%) when the dye concentration is 7.5 ppm when the chemical concentration and pressure are changed.

statistical technique that offers diagnostic tests and statistical results, enabling researchers to evaluate the efficacy of created models. The experimental data and variable symbols are shown in Table 2. In order to determine the necessary operating parameters, a number of tests were carried out using the ultrafiltration membrane technique, each of which changed a single component while maintaining the same values for the other variables.

The aim of the optimization technique known as Response Surface Methodology was for investigating the impact of different parameters (predictors) on the flux and rejection percentage process. The specific information on the historical data of the 20 runs is provided in Table 3. These data points are utilized as design points for the purpose of modeling and optimizing the flux and rejection of dye. The advantage of historical-data RSM design is that it affords the user the opportunity to define the design points using all or some of the available experimental data. In contrast to other types of designs in RSM, the quantity of design elements that may be provided in historical data design is unlimited [67]

5. Results and discussion

5.1. Membrane filtration

To improve membrane performance, Mixed Matrix Membranes (MMMs) blend polymers with inorganic fillers such as carbon nanotubes, metal-organic frameworks, and zeolites. Here is a summary of their benefits and drawbacks in relation to traditional (pure polymer) membranes. The improved permeability and selectivity are two benefits of mixed matrix membranes. By eliminating the trade-off between permeability and selectivity seen in traditional membranes, inorganic fillers may provide more rapid and selective transport channels. Fillers often strengthen the polymer matrix, improving mechanical and thermal stability and increasing MMMs' resistance to temperature, pressure, and chemical deterioration. MMMs may endure longer in challenging conditions if they have improved fouling and deterioration resistance [85]. Each PES/$BiFeO_3$ membrane exhibited a higher pure water flux (PWF) than the neat membrane. The addition of nano additives substantially impacted the flux characteristics, even with a small amount of $BiFeO_3$ NPs. The findings indicated that the flux of water improved from 22.6 (LMH) for the initial membrane to 32.4 (LMH) when 0.4 % of $BiFeO_3$—NPs were introduced. With the use of $BiFeO_3$—NPs, PWF exhibited a significant increase, and the highest recorded value of 52.5 LMH was achieved for SM3. As mentioned earlier, the rise in PWF was in line with the hydrophilicity measurements, porosity, and pore size of the prepared membrane. The pure water flux dropped after adding 0.4 % ($BiFeO_3$—NPs). The high concentration of $BiFeO_3$ NPs has resulted in the blockage of the pore, leading to a decrease in PWF [87].

5.2. Regression equation, ANOVA, and predicted fitted line plot

ANOVA analyses were carried out using Design-Expert®. Tables 4 and 5 show the analysis of variance (ANOVA) findings for the flow and rejection (%) depending on the $BiFeO_3$ NPs weight percentage, MB dye

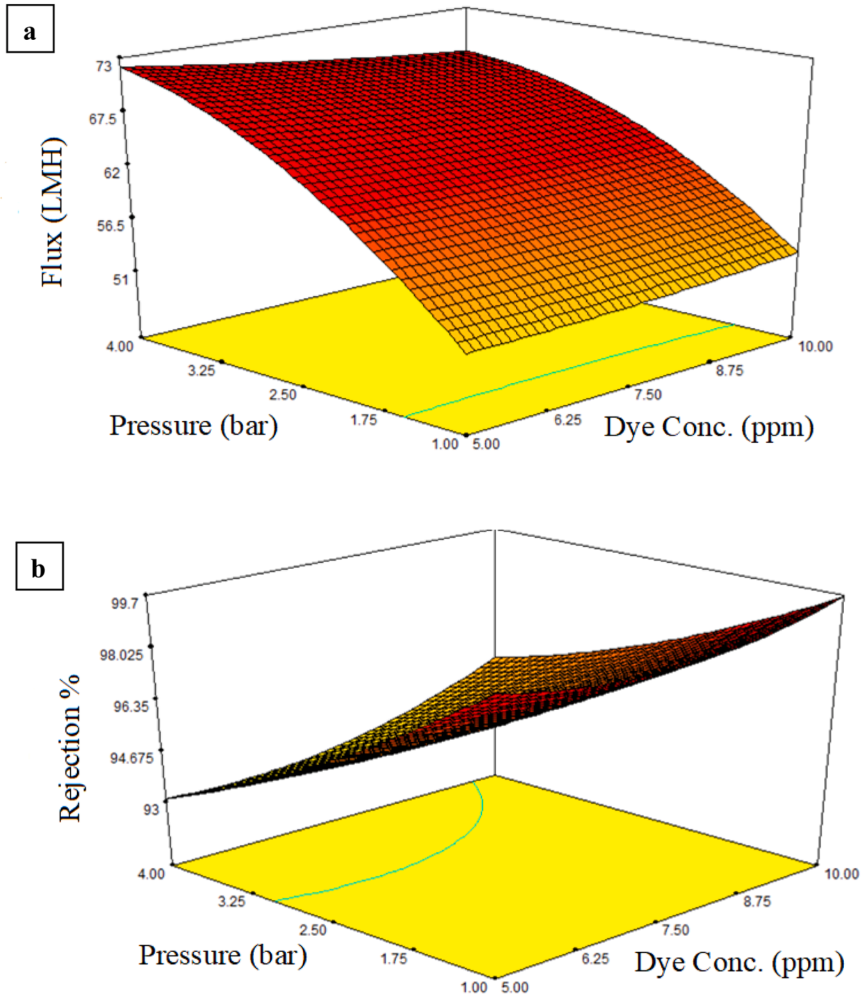

Fig. 8. The influence of pressure and dye concentration on a) membrane permeate flux and b) rejection (%) at an additive concentration of 0.2 wt.%.

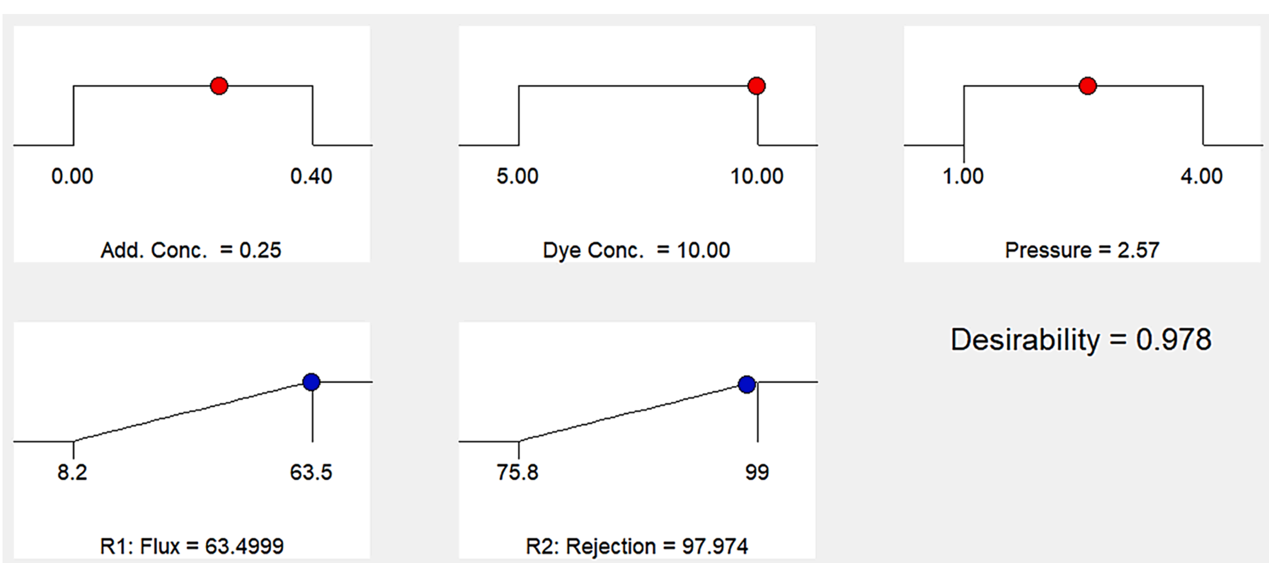

Fig. 9. A desirable ramp is used for numerically optimizing three selected parameters.

concentrations, and transmembrane pressure values. The ANOVA results table includes a particular p-value for each predictor variable in the design arrangement. These findings were used to forecast mathematical equations. Eqs. (9) and 10 for membranes relate the textual form of the regression model equations for flow and rejection (%) about the actual variables.

Table 6
Pred. versus exp. values of the flux and rejection % under optimum conditions.

Add. conc. (wt.%)	Dye conc. (ppm)	Press. (bar)	R. (%) Pred.	R. (%) Exp.	Error %	F(LMH) Pred.	F(LMH) Exp.	Error %
0.25	10	2.57	97.974	96.85	1.16	63.5	64.9	2.15

Table 7
Comparisons between the separation results of membranes in this work and other works in literature.

No.	Membrane	Dye	Dosage wt.%	Rejection %	Flux LMH	Reference
1.	PES/eggshell: SiO_2 (4:1)	Remazol Brilliant Blue R	50	80.38	-	[96]
2.	PSf/TiO_2/MWCNT	Acid black 1	1	99	270	[97]
3.	PSf/Gallium	Reactive blue 4 Rhodamine B	-	66 80	-	[98]
4.	PSf/ACS	MB	7	91.13	1.89	[99]
5.	Am-MSNs/PVDF	RB5	0.6	96.57	23.87	[100]
6.	4A-zeolite/PVA	MB	20	87.41	-	[101]
7.	PES/MOFs	MB MO	5	~ 70 ~ 80	190	[102]
8.	PES/$BiFeO_3$	MB	0.25	97.974	63.5	This work

$$\text{Flux} = +3.35563 + 383.81696\,A - 0.83135\,B + 13.73830\,C + 3.41817\,AB + 10.56878\,AC - 0.33788\,BC - 1038.94379\,A^2 + 0.048970\,B^2 - 1.47560\,C^2 \quad (10)$$

$$\text{Rejection (\%)} = +93.18892 + 124.60550\,A - 1.59898\,B - 5.17221\,C - 1.06515\,AB + 7.50549\,AC + 0.11795\,BC - 244.42064\,A^2 + 0.11727B^2 + 0.20163\,C^2 \quad (11)$$

Where A is the $BiFeO_3$—NPs wt.%., B is the MB dye concentration (ppm), and C is the transmembrane pressure (bar). Negative factor terms indicate their negative influence on the flux, while positive factor terms indicate their positive impact in Eq. (9). A positive indication in the factor term in Eq. (10) indicates a positive impact, while a negative sign indicates a negative impact on the rejection. The correlation coefficient R-Squared values of the flux and rejection% models were 99.79 % and 99.59 %, respectively. On top of that, the results were 99.06 % and 98.25 %, respectively, for the corrected R-Squared. It is appropriately increased and strongly agrees with the values of R-Squared. These results show that the flow and rejection% models are statistically reliable and appropriately predict UF membrane performance. The model's accuracy is demonstrated by the regression analysis of the permeate flux and rejection% models, which is quite precise in its fit with the information provided [88].

Tables 4 and 5 show that the projected correlation coefficient R-Squared (pred.) values nearly match the adjusted correlation coefficient R-Squared for each model. As a result, both mathematical models contained crucial terms.

The flux and rejection % were predicted to use a linear regression function in the Design-Expert® software. Fig. 2.a. depicts the predicted and actual findings for the flux of permeate and rejection of dye %. Thus, the membrane flux and rejection % of actual and predicted values are in strong mathematical agreement as shown in Figs. 2.b. The above finding and the high R-Squared (i.e., 99.79 % and 99.59 % of flux and rejection %) of the PES membrane show the model's significant potential for predicting and optimizing flux and rejection percentages [89]. Also, Table 3 shows that approximately all the predicted values fall within the ±7.29 % and ±1.64 error margins for flux and rejection % respectively.

5.3. Main effects plot

The impact of the experimental parameters and their interactions is analyzed by Design-Expert® software, as illustrated in Figs. 3, 4, and 5. The impact of the factor was investigated by altering one variable, while the others were left unaltered. A zero slope suggests that the variable has grace effect when the factor is adjusted from low to high level. However, a slope of one suggests that the variable has a positive effect on the response.

Fig. 3.a. illustrates that the flux increased as the additive concentration increased by 0.2 wt.%. The membrane's porosity, average pore size, and hydrophilicity were improved by increasing the concentration of $BiFeO_3$ in the PES cast solution. Conversely, the flux was reduced as a result of the $BiFeO_3$ NPs agglomeration on the membrane surface, which led to a decrease in porosity, pore size, and hydrophilicity, when the additive content was increased to 0.4 wt.%. Additionally, the impact of additive concentration on membrane flux and rejection percentage is illustrated in Fig. 3.b., which shows the effect of constant MB dye concentration at 7.5 ppm and 2.5 bar pressure [90].

The rejection percentage for membranes increased as the additive concertation increased. This tendency may have been associated with hydrophilic $BiFeO_3$—NPs, which enhance the hydrophilicity of the membrane surface. Additionally, the percentage of MB dye that was rejected decreased as the concentration of $BiFeO_3$—NPs increased to 0.4 wt.%.

The relationship between flux and rejection (%) for membranes with a constant transmembrane pressure (2.5 bar) and a 0.2 wt.% additive concentration is shown in Fig. 4.a and b., respectively. As the concentration of dye increased (5–12.5 ppm), the flux decreased. The flux decreased due to dye molecules accumulation over the membrane. Meanwhile, the membrane's rejection rate (%) increased as the dye concentration increased from 5 to 12.5 ppm. The total rejection rate can be increased by the formation of a thin, compact coating over the membrane surface due to the presence of dye molecules [91,92].

Fig. 5. a and b. show how adjusting the pressure from one to four bars impacts the flow and % membranes rejection, at a constant MB dye concentration of 7.5 ppm and additive concentration of 0.2 wt.%. Flux increased as the pressure increased from 1 to 4 bar. With the diffusion and solution model, flux has a direct connection with the pressure differential through the membrane. But the rejection % for membrane decreased slightly as the pressure rose from 1 to 4 bar.

5.4. Effect of $BiFeO_3$ additives concentration, MB dye concentration and pressure, on flux and rejection %

The dye response flux and rejection percentage may be shown as a three-dimensional solid. Figs. 6, 7, and 8 show the permeate flux and MB dye rejection % with the two parameters. The primary goal of the response surface plot aims to determine the optimal operation factors, which can be expressed by the additives conc. (wt.%), dye concentration and pressure, resulting in the maximum flux of permeate and rejection % for the dye.

The permeate flux at a constant pressure is illustrated by a response surface diagram in Fig. 6.a, which depicts the effect of dye concentration and additive content. A decrease in the dye concentration and an increase in the additive concentration to 0.2 wt.% were shown to result in a higher flux in the permeate flux response. With 0.2 wt.% of $BiFeO_3$—NPs added, the highest flux was observed over 52.5 LMH. The membrane's porosity, average pore size, and hydrophilicity were improved by increasing the concentration of $BiFeO_3$—NPs in the PES cast solution. Conversely, increasing the additive concentration to 0.4 wt.% decreased the flow owing to the aggregation of additives on the surface of PES membranes, leading to reduced porosity, pore size, and hydrophilicity. Furthermore, the MB dye rejection dropped to around 92 % when the $BiFeO_3$—NPs concentration increased to 0.4 wt percent. A significant quantity of $BiFeO_3$—NP aggregation may be the cause of the decrease in dye rejection. The proportion of membrane rejection may suffer as a result of the sporadic defects that are created throughout the membrane manufacturing process. Similar results have also been reported by researchers, suggesting that increasing the concentration of nanofillers results in a reduction in dispersion within the polymer matrix and the production of agglomerates. The observed decrease in rejection might be explained by this phenomenon [93]. As shown in Fig. 6.b, the dye rejection% response showed that lowering the dye concentration and increasing the additive amount to 0.2 wt.% produced a smaller rejection% at constant pressure. Plotting of elliptical contours shows interaction between additive amount and dye feed concentration.

At a constant dye concentration of 7.5 ppm, Fig. 7.a. illustrates the three-dimensional plot of the response surface, which illustrates the impact of the coupling of the interaction between the additive concentration and the pressure on the permeate flux. The permeate flux increased more than the pressure when the additive content increased to 0.4 wt.%. The permeate flux is generally increased as a result of the combined effect of increasing the $BiFeO_3$ NPs content in the PES solution, increasing the hydrophilicity, average pore size, and porosity of the membrane, and increasing the pressure. This is due to the higher shear stress on the membrane's surface [94,96].

Fig. 7.b. shows a response surface plot that also shows how the amount of additives and pressure affect the rejection rate when the dye content stays the same. The rejection was improved by increasing the additive concentration to 0.2 wt.%, while the rejection was decreased by increasing the pressure. Nevertheless, the rejection was improved, even under high pressure, when the additive concentration was increased to 0.4 wt.%. Furthermore, the contour plots' elliptical shape results in a discernible interaction between the additive concentration and the pressure.

The response surface diagram, depicted in Fig. 8.a., illustrates the impact of dye concentration and pressure on the permeate flux. The permeate flux is diminished when the dye concentration increases, and the pressure is decreased. The flux was significantly reduced by a decrease in pressure from 4 to 1, while a minor decrease in flux was the result of a rise in the dye concentration, which was less effective than the pressure. The dye rejection percentage is also influenced by the pressure and dye concentration, as illustrated in Fig. 8.b. response surface plot. The rejection rate was adversely affected by the slight decrease in membrane rejection that resulted from the increase in pressure. Consequently, the rejection rate decreased at higher pressures, while the rejection percentage increased as the pigment concentration increased. The dye molecules on the membrane surface can generate a narrow, compact layer, which in turn increases the total rejection rate, which is the cause of the increase in rejection. Nevertheless, the parallel straight lines structure of the contour maps is the reason for the lack of interaction between these factors.

5.5. Validity and optimization of the UF procedure

One of the most prominent methods for optimizing a variety of response processes in the applied engineering and science domains is the desired function technique. The method integrates the responses to individual desirability from a singular value within a scale that spans from one to zero. The optimal conditions for operation are established by selecting values that are closest to one, as one value represents the optimum scenario. Conversely, when the outcome is near zero, all or a portion of the responses are outside the intended range [95]. The desirability function for the two present responses (flux and rejection %) was determined using Design-Expert® software, which integrated the individual desirability into a single value, as illustrated in Fig. 9. The optimal operating conditions tested (i.e., MB dye concentration, pressure, and additive concentration) are depicted in the accompanying figure, as it was estimated that the three variables would substantially improve the permeate flux and rejection factor. Additionally, the model was validated by conducting the flux and rejection % experiments at the optimal operation conditions that were recommended. Table 6 indicates a 2.15 % discrepancy between the experimental value (64.9 LMH) and the predicted flux (63.5 LMH) for membranes. Furthermore, the experimental value (96.85) was 1.16 % lower than the predicted rejection rate (97.974). The significance and applicability of the RSM model that was developed are demonstrated by the minor percentage error. To highlight the novelty of the present work, Table 7 shows the comparison between the results found in this work and the other works.

5.6. Development prospects

The worldwide demands for energy efficiency, environmental sustainability, and innovative materials have led to notable improvements in the area of membrane separation, but there is still a great deal of room for further optimization. The growth potential may be examined from a number of important angles: Designing and preparing new membrane materials is one of the most promising approaches. This includes mixed matrix membranes (MMMs), and nanocomposite membranes. Enhancing permeability, selectivity, and resistance to fouling or deterioration is the goal of these developments. There may be synergistic advantages to combining membrane separation with other methods. More accurate forecasts of membrane performance are now possible because of developments in computational tools such as machine learning, process modelling software, and molecular dynamics simulations. These technologies are critical for optimizing membrane designs under practical operating circumstances and speeding up development cycles. High-performance membrane manufacture on a commercial scale is still difficult. To guarantee long-term sustainability, opportunities include the creation of recyclable or biodegradable membranes, green production techniques, and enhanced lifetime evaluations. Overall, there are a lot of exciting opportunities for membrane separation optimization advancement, driven by both basic research and business demands. The next generation of high-performance membrane systems will probably be developed via multidisciplinary cooperation, where material science, engineering, and data science come together.

6. Conclusion

A new polyethersulfone (PES) membrane was produced through the implementation of a phase inversion method. To improve the membrane's characteristics, including permeability, selectivity and resistance to contamination, hydrophilic additives of novel $BiFeO_3$ NPs were introduced to the majority of the PES membrane. Based on the positive outcomes from this study, employing $BiFeO_3$ NPs was strongly advised nanocomposite ultrafiltration membranes to eliminate MB dye.

Variance analysis (ANOVA) and response surface methodology (RSM) have been applied as mathematical and statistical tools to raise the general effectiveness of the approach. The impact of operational variables on the permeate flux and rejection of MB dye of PES/$BiFeO_3$ membranes in the ultrafiltration technique was investigated in an optimization sense. The factors shown to have the most impact on the flux and rejection of oil were transmembrane pressure, oil concentration, and $BiFeO_3$ NPs wt.%. The effects of three MB dye feed solution concentrations may be investigated thanks to the experimental design. Design-Expert® software was used to analyze the flow and rejection percentage. A mathematical approach was created to calculate the rejection percentage and flow. The results show that a combination of factors affect both rejection percentage and flux. With an Add. conc (wt.%) of 0.25, a dye concentration of 10 ppm, and a pressure of 2.57 bar, the optimized parameters show that the membrane flux is 63.5 LMH and the rejection percentage is 97.974.

CRediT authorship contribution statement

Shahad K. Jawad: Writing – original draft, Investigation, Formal analysis, Data curation, Conceptualization. **Khalid T. Rashid:** Writing – review & editing, Writing – original draft, Supervision, Investigation, Formal analysis, Data curation, Conceptualization. **Manal Afham Toma:** Writing – original draft, Supervision, Investigation, Formal analysis, Data curation, Conceptualization. **Adnan A. Abdul Razak:** Writing – review & editing, Writing – original draft, Software, Methodology, Investigation, Formal analysis, Data curation, Conceptualization. **Mohammed Ahmed Shehab:** Writing – review & editing, Writing – original draft, Resources, Methodology, Investigation. **Maryam Y. Ghadhban:** Resources, Investigation, Formal analysis. **Munaf Al-lami:** Visualization, Investigation, Formal analysis. **Alhafadhi Mahmood:** Writing – original draft, Formal analysis. **Haidar Hasan Mohammed:** Validation, Investigation, Formal analysis. **Amaal Ajeel Hmood:** Resources, Investigation, Formal analysis. **Mohammed Faleh Abd Al-Ogaili:** Visualization, Resources, Investigation, Formal analysis. **Saad Alsarayefi:** Resources, Investigation, Formal analysis.

Declaration of competing interest

The authors declare that they have no known competing financial interests or personal relationships that could have appeared to influence the work reported in this paper.

Data availability

Data will be made available on request.

References

[1] D. Qadir, H. Mukhtar, L.K. Keong, Mixed matrix membranes for water purification applications, Sep. Purif. Rev. 46 (1) (2017) 62–80, https://doi.org/10.1080/15422119.2016.1196460.
[2] S. Bassim, A.K. Mageed, A.A. AbdulRazak, F. Al-Sheikh, Photodegradation of methylene blue with aid of green synthesis of CuO/TiO_2 nanoparticles from extract of citrus aurantium juice, Bull. Chem. React. Eng. Catal. 18 (1) (2023) 1–16, https://doi.org/10.9767/bcrec.16417.
[3] F.S. Ahmed, M.A. Alsaffar, A.A. AbdulRazak, One-step synthesis of magnetic fly ash composites for methylene blue removal: batch and column study, Env. Sci. Pollut. Res. Int. 30 (60) (2023) 124748–124766, https://doi.org/10.1007/s11356-022-23491-x.
[4] H. Zollinger, Color Chemistry : syntheses, Properties, and Applications of Organic Dyes and Pigments, 2nd rev. ed, VCH, Weinheim, 1991.
[5] Q. Du, J. Sun, Y. Li, X. Yang, X. Wang, Z. Wang, L. Xia, Highly enhanced adsorption of congo red onto graphene oxide/chitosan fibers by wet-chemical etching off silica nanoparticles, Chem. Eng. J. 245 (2014) 99–106, https://doi.org/10.1016/j.cej.2014.02.006.
[6] H. Jain, R. Dhupper, A.K. Verma, M.C. Garg, Development of titanium dioxide incorporated ultrathin cellulose acetate membrane for enhanced forward osmosis performance, Nanotechnol. Environ. Eng. 6 (2021) 1–8, https://doi.org/10.1007/s41204-021-00161-w.
[7] H. Patel, R.T. Vashi, Removal of Congo red dye from its aqueous solution using natural coagulants, J. Saudi Chem. Soc. 16 (2) (2012) 131–136, https://doi.org/10.1016/j.jscs.2010.12.003.
[8] Q. Li, Q.-Y. Yue, H.-J. Sun, Y. Su, B.-Y. Gao, A comparative study on the properties, mechanisms and process designs for the adsorption of non-ionic or anionic dyes onto cationic-polymer/bentonite, J. Env. Manage. 91 (7) (2010) 1601–1611, https://doi.org/10.1016/j.jenvman.2010.03.001.
[9] M.A.M. Salleh, D.K. Mahmoud, W.A.W.A. Karim, A. Idris, Cationic and anionic dye adsorption by agricultural solid wastes: a comprehensive review, Desalination 280 (2011) 1–13, https://doi.org/10.1016/j.desal.2011.07.019.
[10] M.K. Purkait, A. Maiti, S. Das Gupta, S. De, Removal of Congo Red using activated carbon and its regeneration, J. Hazard. Mater. 145 (1–2) (2007) 287–295, https://doi.org/10.1016/j.jhazmat.2006.11.021. Issues.
[11] M.F. Attallah, I.M. Ahmed, M.M. Hamed, Treatment of industrial wastewater containing Congo Red and Naphthol Green B using low-cost adsorbent, Env. Sci. Pollut. Res. 20 (2013) 1106–1116, https://doi.org/10.1007/s11356-012-0947-4.
[12] S. Abo-Farha, Comparative study of oxidation of some azo dyes by different advanced oxidation processes: fenton, fenton-like, photo-fenton and photo-fenton-like, J. Am. Sci. 6 (10) (2010) 128–142.
[13] A.K. Verma, R.R. Dash, P. Bhunia, A review on chemical coagulation/flocculation technologies for removal of colour from textile wastewaters, J. Env. Manage. 93 (1) (2012) 154–168, https://doi.org/10.1016/j.jenvman.2011.09.012.
[14] V. Munagapati, D.-S. Kim, Adsorption of anionic azo dye Congo Red from aqueous solution by cationic modified orange peel powder, J. Mol. Liq. 220 (2016) 540–548, https://doi.org/10.1016/j.molliq.2016.04.119.
[15] F.S. Ahmed, A.A. Abdulrazak, M.A. Alsaffar, Modelling and optimization of methylene blue adsorption from wastewater utilizing magnetic marble dust adsorbent: a response surface methodology approach, Mater. Today Proc. 60 (2022) 1676–1688, https://doi.org/10.1016/j.matpr.2021.12.224.
[16] M.-X. Zhu, L. Lee, H.-H. Wang, Z. Wang, Removal of an anionic dye by adsorption/precipitation processes using alkaline white mud, J. Hazard. Mater. 149 (3) (2007) 735–741, https://doi.org/10.1016/j.jhazmat.2007.04.037.
[17] S. Chakraborty, B. Basak, S. Dutta, B. Bhunia, A. Dey, Decolorization and biodegradation of congo red dye by a novel white rot fungus alternaria alternata CMERI F6, Bioresour. Technol. 147 (2013) 662–666, https://doi.org/10.1016/j.biortech.2013.08.117.
[18] M.I. Khan, S. Akhtar, S. Zafar, A. Shaheen, M.A. Khan, R. Luque, A.U. Rehman, Removal of Congo red from aqueous solution by Anion Exchange membrane (EBTAC): adsorption kinetics and themodynamics, Material 8 (2015) 4147–4161, https://doi.org/10.3390/ma8074147.
[19] Y. Jia, L. Ding, P. Ren, M. Zhong, J. Ma, X. Fan, Performances and mechanism of Methyl orange and Congo red adsorbed on the magnetic ion-exchange resin, J. Chem. Eng. Data 65 (2) (2020) 725–736, https://doi.org/10.1021/acs.jced.9b00951.
[20] A. Akhtar, Z. Aslam, A. Asghar, M.M. Bello, A.A.A. Raman, Electrocoagulation of Congo red dye-containing wastewater: optimization of operational parameters and process mechanism, J. Environ. Chem. Eng. 8 (5) (2020) 104055, https://doi.org/10.1016/j.jece.2020.104055.
[21] U. Habiba, T.A. Siddique, T.C. Joo, A. Salleh, B. Chin Ang, A.M. Afifi, Synthesis of chitosan/polyvinyl alcohol/zeolite composite for removal of methyl orange, Congo red and chromium(VI) by flocculation/adsorption, Carbohydr. Polym. 157 (2017) 1568–1576, https://doi.org/10.1016/j.carbpol.2016.11.037.
[22] G. Han, Y. Du, Y. Huang, W. Wang, S. Su, B. Liu, Study on the removal of hazardous Congo red from aqueous solutions by chelation flocculation and precipitation flotation process, Chemosphere 289 (2022) 133109, https://doi.org/10.1016/j.chemosphere.2021.133109.
[23] M.A. Shannon, P.W. Bohn, M. Elimelech, J.G. Georgiadis, B.J. Mariñas, A. M. Mayes, Science and technology for water purification in the coming decades, Nature 452 (2008) 301–310, https://doi.org/10.1038/nature06599.
[24] M.E. Haddad, R. Slimani, R. Mamouni, S.E. Antri, S. Lazar, Removal of two textile dyes from aqueous solutions onto calcined bones, J. Associ. Arab Uni. Appl. Sci. 14 (1) (2013) 51–59, https://doi.org/10.1016/j.jaubas.2013.03.002.
[25] C. Lim, N. Kim, J. Lee, Y. Yoon, Comparative evaluation of cationic and anionic dye removal using graphene oxide fabricated by Hummers and Couette-Taylor flow methods, Carbon Trends 19 (2025) 100476, https://doi.org/10.1016/j.cartre.2025.100476.
[26] M. Nadeem Zafar, Q. Dar, F. Nawaz, M. Naveed Zafar, M. Iqbal, M.F. Nazar, Effective adsorptive removal of azo dyes over spherical ZnO nanoparticles, J. Mater. Res. Technol. 8 (1) (2019) 713–725, https://doi.org/10.1016/j.jmrt.2018.06.002.
[27] P. Gharbani, Modeling and optimization of reactive yellow 145 dye removal process onto synthesized MnO_X -CeO_2 using response surface methodology, Colloids Surf. A: Physicochem. Eng. Asp. 548 (2018) 191–197, https://doi.org/10.1016/j.colsurfa.2018.03.046.
[28] S. Kucukcongar, A.G.J. Alwindawi, M. Turkyilmaz, I. Ozaytekin, Reactive dye removal by photocatalysis and sonophotocatalysis processes using $Ag/TiO_2/Fe_3O_4$ nanocomposite, Water. Air. Soil. Pollut. 234 (2023) 103, https://doi.org/10.1007/s11270-023-06136-8.
[29] E. Fathi, F. Derakhshanfard, P. Gharbani, Z. Ghazi Tabatabaei, Facile synthesis of MgO/C_3N_4 nanocomposite for removal of reactive orange 16 under visible light, J. Inorg. Organomet. Polym. Mater. 30 (6) (2019) 2234–2240, https://doi.org/10.1007/s10904-019-01362-2.
[30] M.A. Shehab, G. Karacs, T. Koós, N. Sharma, K. Hernádi, Z. Németh, Adsorptive removal of methylene blue by TiO_2 nanowire/Fe_2O_3 nanocomposite, Circ. Econ. and Environ. Prot. 5 (2) (2021) 16–28.
[31] P. Beirami, F. Derakhshanfard, P. Gharbani, L. Amirkhani, Visible-light photocatalytic removal of betamethasone using heterogeneous $CdSe/Bi_2MoO_6/g$-C_3N_5 nanophotocatalyst: synthesis, characterization, thermodynamic and kinetics analysis, J. Photochem. Photobiol. A: Chem. 444 (2023) 114910, https://doi.org/10.1016/j.jphotochem.2023.114910.
[32] B.H. Fard, R.R. Khojasteh, P. Gharbani, Preparation and characterization of visible-light sensitive nano $Ag/Ag_3VO_4/AgVO_3$ modified by graphene oxide for photodegradation of reactive orange 16 dye, J. Inorg. Organomet. Polym. Mater. 28 (3) (2018) 1149–1157, https://doi.org/10.1007/s10904-018-0798-7.
[33] A. Eteba, M. Bassyouni, M.H. Elzahar, M.Z. El-Shekhib, Development of a sustainable multilayer chitosan-based nanocomposite membrane for effective

removal of DB78 dye from aqueous solution, Results Eng. 25 (2025) 104248, https://doi.org/10.1016/j.rineng.2025.104248.
[34] U. Yanuhar, H. Suryanto, M.A.M.T. Mohamad Lal, J. Maulana, N. Rahman Caesar, The impact of copper oxide nanoparticles reinforced nanocellulose acetate membrane on antibacterial and dye removal potency, Results Eng. 23 (2024) 102788, https://doi.org/10.1016/j.rineng.2024.102788.
[35] A. Sutedja, C.A. Josephine, D. Mangindaan, Polysulfone thin film composite nanofiltration membranes for removal of textile dyes wastewater, IOP Conf. Ser.: Earth Environ. Sci. 109 (2017) 012042, https://doi.org/10.1088/1755-1315/109/1/012042.
[36] T. Robinson, G. McMullan, R. Marchant, P. Nigam, Remediation of dyes in textile effluent: a critical review on current treatment technologies with a proposed alternative, Bioresour. Technol. 77 (3) (2001) 247–255, https://doi.org/10.1016/S0960-8524(00)00080-8.
[37] M. Riera-Torres, C. Gutiérrez-Bouzán, M. Crespi, Combination of coagulation–flocculation and nanofiltration techniques for dye removal and water reuse in textile effluents, Desalination 252 (1) (2010) 53–59, https://doi.org/10.1016/j.desal.2009.11.002.
[38] B. Tansel, New technologies for water and wastewater treatment: a survey of recent patents, Recent Pat. Chem. Eng. 1 (1) (2008) 17–26, https://doi.org/10.2174/1874478810801010017.
[39] K. Singh, S. Arora, Removal of synthetic textile dyes from wastewaters: a critical review on present treatment technologies, Crit. Rev. Env. Sci. Technol. 41 (9) (2011) 807–878, https://doi.org/10.1080/10643380903218376.
[40] K. Majewska-Nowak, Ultrafiltration of dye solutions in the presence of cationic and anionic surfactants, Environ. Prot. Eng. 35 (2009) 111–121.
[41] R. Zhang, Y. Liu, M. He, Y. Su, X. Zhao, M. Elimelech, Z. Jiang, Antifouling membranes for sustainable water purification: strategies and mechanisms, Chem. Soc. Rev. 45 (2016), https://doi.org/10.1039/C5CS00579E.
[42] M. Amini, M. Arami, N. Mohammad Mahmoodi, A. Akbari, Dye removal from colored textile wastewater using acrylic grafted nanomembrane, Desalination 267 (1) (2011) 107–113, https://doi.org/10.1016/j.desal.2010.09.014.
[43] T.A. Nguyen, R.-S. Juang, Treatment of waters and wastewaters containing sulfur dyes: a review, Chem. Eng. J. 219 (2013) 109–117, https://doi.org/10.1016/j.cej.2012.12.102.
[44] J. Dasgupta, J. Sikder, S. Chakraborty, S. Curcio, E. Drioli, Remediation of textile effluents by membrane based treatment techniques: a state of the art review, J. Env. Manage. 147 (2015) 55–72, https://doi.org/10.1016/j.jenvman.2014.08.008.
[45] R.S. Hebbar, A.M. Isloor, A.K. Zulhairun, M.S. Abdullah, A.F. Ismail, Efficient treatment of hazardous reactive dye effluents through antifouling polyetherimide hollow fiber membrane embedded with functionalized halloysite nanotubes, J. Taiwan Inst. Chem. Eng. 72 (2017) 244–252, https://doi.org/10.1016/j.jtice.2017.01.022.
[46] Y. Zhan, X. Wan, S. He, Q. Yang, Y. He, Design of durable and efficient poly (arylene ether nitrile)/bioinspired polydopamine coated graphene oxide nanofibrous composite membrane for anionic dyes separation, Chem. Eng. J. 333 (2018) 132–145, https://doi.org/10.1016/j.cej.2017.09.147.
[47] H.P. Srivastava, G. Arthanareeswaran, N. Anantharaman, V.M. Starov, Performance of modified poly(vinylidene fluoride) membrane for textile wastewater ultrafiltration, Desalination 282 (2011) 87–94, https://doi.org/10.1016/j.desal.2011.05.054.
[48] M.A. Abdel-Fatah, Nanofiltration systems and applications in wastewater treatment: review article, Ain Shams Eng. J. 9 (4) (2018) 3077–3092, https://doi.org/10.1016/j.asej.2018.08.001.
[49] R.M. Al-Maliki, Q.F. Alsalhy, S. Al-Jubouri, A.A. Abdul Razak, M.A. Shehab, Z. Németh, K. Hernadi, H.S. Majdi, Enhanced antifouling in flat-sheet polyphenylsulfone membranes incorporating graphene oxide–Tungsten oxide for ultrafiltration applications, Membranes 13 (2023) 269, https://doi.org/10.3390/membranes13030269.
[50] A. Karunakaran, A.A. Mungray, S. Agarwal, M.C. Garg, Optimization of the forward-osmosis performance with a low-concentration draw solution using response surface modeling, Chem. Eng. Technol. 44 (7) (2021) 1278–1286, https://doi.org/10.1002/ceat.202000453.
[51] I. Petrinić, N.P.R. Andersen, S. Šostar-Turk, A.M.L. Marechal, The removal of reactive dye printing compounds using nanofiltration, Dyes Pigm. 74 (3) (2007) 512–518, https://doi.org/10.1016/j.dyepig.2006.11.003.
[52] R.J. Petersen, Composite reverse osmosis and nanofiltration membranes, J. Memb. Sci. 83 (1) (1993) 81–150, https://doi.org/10.1016/0376-7388(93)80014-O.
[53] M.M. Pendergast, E.M.V. Hoek, A review of water treatment membrane nanotechnologies, Energy Env. Sci. 4 (6) (2011) 1946–1971, https://doi.org/10.1039/C0EE00541J.
[54] P.S. Kumar, K. Venkatesh, E.L. Gui, J. Sundaramurthy, G. Singh, G. Arthanareeswaran, Electrospun carbon nanofibers/TiO_2-PAN hybrid membranes for effective removal of metal ions and cationic dye, Environ. Nanotechnol. Monit. Manag. 10 (2018) 366–376, https://doi.org/10.1016/j.enmm.2018.08.006.
[55] J. Lin, C.Y. Tang, W. Ye, S.-P. Sun, S.H. Hamdan, A. Volodin, C.V. Haesendonck, A. Sotto, P. Luis, B. Van der Bruggen, Unraveling flux behavior of superhydrophilic loose nanofiltration membranes during textile wastewater treatment, J. Memb. Sci. 493 (2015) 690–702, https://doi.org/10.1016/j.memsci.2015.07.018.
[56] E. Bagheripour, A.R. Moghadassi, S.M. Hosseini, Fabrication of polyvinyl chloride based nanocomposite nanofiltration membrane: investigation of SDS/Al_2O_3 nanoparticle concentration and solvent ratio effects, Asia-Pac. J. Chem. Eng. 10 (5) (2015) 791–798, https://doi.org/10.1002/apj.1918.
[57] M.-B. Wu, Y. Lv, H.-C. Yang, L.-F. Liu, X. Zhang, Z.-K. Xu, Thin film composite membranes combining carbon nanotube intermediate layer and microfiltration support for high nanofiltration performances, J. Memb. Sci. 515 (2016) 238–244, https://doi.org/10.1016/j.memsci.2016.05.056.
[58] F. Liu, B.-R. Ma, D. Zhou, L.-J. Zhu, Y.-Y. Fu, L.-X. Xue, Positively charged loose nanofiltration membrane grafted by diallyl dimethyl ammonium chloride (DADMAC) via UV for salt and dye removal, React. Funct. Polym. 86 (2015) 191–198, https://doi.org/10.1016/j.reactfunctpolym.2014.09.003.
[59] Q. Xie, S. Zhang, Z. Xiao, X. Hu, Z. Hong, R. Yi, W. Shao, Q. Wang, Preparation and characterization of novel alkali-resistant nanofiltration membranes with enhanced permeation and antifouling properties: the effects of functionalized graphene nanosheets, RSC Adv. 7 (30) (2017) 18755–18764, https://doi.org/10.1039/C7RA00928C.
[60] H. Susanto, M. Ulbricht, Characteristics, performance and stability of polyethersulfone ultrafiltration membranes prepared by phase separation method using different macromolecular additives, J. Memb. Sci. 327 (1) (2009) 125–135, https://doi.org/10.1016/j.memsci.2008.11.025.
[61] A. Asad, D. Sameoto, M. Sadrzadeh, Chapter 1 - overview of membrane technology, Nanocomposite membranes for water and gas separation, Micro. Nano Technol. (2020) 1–28, https://doi.org/10.1016/B978-0-12-816710-6.00001-8.
[62] H. Jain, A. Kumar, A.K. Verma, S. Wadhwa, V.D. Rajput, T. Minkina, M.C. Garg, Treatment of textile industry wastewater by using high-performance forward osmosis membrane tailored with alpha-manganese dioxide nanoparticles for fertigation, Environ. Sci. Pollut. Res. 29 (53) (2022) 80032–80043, https://doi.org/10.1007/s11356-022-20047-x.
[63] T. Saleh, V. Gupta, Membrane classification and Membrane operations, Nanomater. Polym. Membr. Synth. Charact. Appl. (2016) 55–82, https://doi.org/10.1016/B978-0-12-804703-3.00003-6.
[64] H. Koulivand, A. Shahbazi, V. Vatanpour, M. Rahmandoust, Development of carbon dot-modified polyethersulfone membranes for enhancement of nanofiltration, permeation and antifouling performance, Sep. Purif. Technol. 230 (2020) 115895, https://doi.org/10.1016/j.seppur.2019.115895.
[65] M. Abdullah, S. Al-Jubouri, Implementation of hierarchically porous zeolite-polymer membrane for chromium ions removal, IOP Conf. Ser.: Earth Environ. Sci. 779 (1) (2021) 012099, https://doi.org/10.1088/17551315/779/1/012099.
[66] N. Nasrollahi, V. Vatanpour, S. Aber, N.M. Mahmoodi, Preparation and characterization of a novel polyethersulfone (PES) ultrafiltration membrane modified with a CuO/ZnO nanocomposite to improve permeability and antifouling properties, Sep. Purif. Technol. 192 (2017) 369–382, https://doi.org/10.1016/j.seppur.2017.10.034.
[67] A. Karunakaran, A.A. Mungray, M.C. Garg, Effects of temperature, pH, feed, and fertilizer draw solution concentrations on the performance of forward osmosis process for textile wastewater treatment, Water Environ. Res. 93 (10) (2021) 2329–2340, https://doi.org/10.1002/wer.1607.
[68] D. Zhang, A. Karkooti, L. Liu, M. Sadrzadeh, T. Thundat, Y. Liu, R. Narain, Fabrication of antifouling and antibacterial polyethersulfone (PES)/cellulose nanocrystals (CNC) nanocomposite membranes, J. Memb. Sci. 549 (2018) 350–356, https://doi.org/10.1016/j.memsci.2017.12.034.
[69] B. Van der Bruggen, B. Daems, D. Wilms, C. Vandecasteele, Mechanisms of retention and flux decline for the nanofiltration of dye baths from the textile industry, Sep. Purif. Technol. 22-23 (2001) 519–528, https://doi.org/10.1016/S1383-5866(00)00134-9.
[70] B. Van der Bruggen, G. Cornelis, C. Vandecasteele, I. Devreese, Fouling of nanofiltration and ultrafiltration membranes applied for wastewater regeneration in the textile industry, Desalination 175 (1) (2005) 111–119, https://doi.org/10.1016/j.desal.2004.09.025.
[71] A. Al-Amoudi, R.B. Lovitt, Fouling strategies and the cleaning system of NF membranes and factors affecting cleaning efficiency, J. Memb. Sci. 303 (2007) 4–28, https://doi.org/10.1016/j.memsci.2007.06.002.
[72] W. Zhang, W. Liang, Z. Zhang, Dynamic scouring of multifunctional granular material enhances filtration performance in membrane bioreactor: mechanism and modeling, J. Memb. Sci. 663 (2022) 120979, https://doi.org/10.1016/j.memsci.2022.120979.
[73] M. Safarpour, V. Vatanpour, A. Khataee, Preparation and characterization of graphene oxide/TiO_2 blended PES nanofiltration membrane with improved antifouling and separation performance, Desalination 393 (2016) 65–78, https://doi.org/10.1016/j.desal.2015.07.003.
[74] V. Vatanpour, S.S. Madaeni, R. Moradian, S. Zinadini, B. Astinchap, Fabrication and characterization of novel antifouling nanofiltration membrane prepared from oxidized multiwalled carbon nanotube/polyethersulfone nanocomposite, J. Memb. Sci. 375 (1) (2011) 284–294, https://doi.org/10.1016/j.memsci.2011.03.055.
[75] M. Mosadegh, H. Mahdavi, Synthesis and characterization of novel PES/GO-g-PSS mixed matrix membranes with outstanding antifouling and dye rejection properties, J. Iran. Chem. Soc. 18 (11) (2021) 2883–2896, https://doi.org/10.1007/s13738-021-02236-6.
[76] W. Zhang, W. Liang, Z. Zhang, T. Hao, Aerobic granular sludge (AGS) scouring to mitigate membrane fouling: performance, hydrodynamic mechanism and contribution quantification model, Water Res. 188 (2021) 116518, https://doi.org/10.1016/j.watres.2020.116518.
[77] N. Asefi, M. Hasheminiasari, S.M. Masoudpanah, Photocatalytic properties of $BiFeO_3$ powders synthesized by the mixture of CTAB and glycine, Sci. Rep. 13 (2023) 12338, https://doi.org/10.1038/s41598-023-39622-4.

[78] J. Luo, P.A. Maggard, Hydrothermal synthesis and photocatalytic activities of $SrTiO_3$-coated Fe_2O_3 and $BiFeO_3$, Adv. Mater. 18 (2006) 514, https://doi.org/10.1002/adma.200500109.
[79] L. Lu, M. Lv, G. Liu, X. Xu, Photocatalytic hydrogen production over solid solutions between $BiFeO_3$ and $SrTiO_3$, Appl. Surf. Sci. 391 (Part B) (2017) 535–541, https://doi.org/10.1016/j.apsusc.2016.06.160.
[80] D. Zhang, C. Boffo, D.C. Dunand, Additively-manufactured monocrystalline YBCO superconductor, Nat. Commun. 16 (2025) 1933, https://doi.org/10.1038/s41467-025-56708-x.
[81] Y. Li, X.-T. Wang, X.-Q. Zhang, X. Li, J. Wang, C.-W. Wang, New hydrothermal synthesis strategy of nano-sized $BiFeO_3$ for high-efficient photocatalytic applications, Phys. E: Low-Dimens. Syst. Nanostruct. 118 (2020) 113865, https://doi.org/10.1016/j.physe.2019.113865.
[82] Q.F. Alsalhy, K.T. Rashid, S.S. Ibrahim, A.H. Ghanim, B. Van der Bruggen, P. Luis, M. Zablouk, Poly (vinylidene fluoride-co-hexafluoropropylene)(PVDF-co-HFP) hollow fiber membranes prepared from PVDF-co-HFP/PEG-600Mw/DMAC solution for membrane distillation, J. Appl. Polym. Sci. 129 (6) (2013) 3304–3313, https://doi.org/10.1002/app.39065.
[83] K.T. Rashid, H.M. Alayan, A.E. Mahdi, M.N. AL-Baiati, H.S. Majdi, I.K. Salih, J. M. Ali, Q.F. Alsalhy, Novel water-soluble poly(terephthalic-co-glycerol-g-fumaric acid) copolymer nanoparticles harnessed as pore formers for polyethersulfone membrane modification: permeability–Selectivity tradeoff manipulation, Water 14 (2022) 1507, https://doi.org/10.3390/w14091507.
[84] M.Y. Ghadhban, K.T. Rashid, A.A. Abdulrazak, I.T. Ibrahim, Q.F. Alsalhy, Z. M. Shakor, I. Hamawand, Modification of polylactide-poly (butylene adipate-co-terephthalate)(PLA/PBAT) mixed-matrix membranes (MMMs) with green banana peel additives for oil wastewater treatment, Water 16 (7) (2024) 1040, https://doi.org/10.3390/w16071040.
[85] A.M. Ali, K.T. Rashid, A.A. Yahya, H.S. Majdi, I.K. Salih, K. Yusoh, Q.F. Alsalhy, A.A. Abdul Razak, A. Figoli, Fabrication of gum Arabic-graphene (GGA) modified polyphenylsulfone (PPSU) mixed matrix membranes: a systematic evaluation study for ultrafiltration (UF) applications, Membranes 11 (2021) 542, https://doi.org/10.3390/membranes11070542.
[86] Z.M. Shakor, A.A. Abdul Razak, A.A. Shuhaib, Optimization of process variables for hydrogenation of cinnamaldehyde to cinnamyl alcohol over a Pt/SiO_2 catalyst using response surface methodology, Chem. Eng. Commun. 209 (6) (2021) 827–843, https://doi.org/10.1080/00986445.2021.1922394.
[87] R.I. Raja, K.T. Rashid, M.A. Toma, A.A. Abdul Razak, M.A. Shehab, K. Hernadi, A novel polyethersulfone/Chamomile (PES/Chm) mixed matrix membranes for wastewater treatment applications, J. Saudi Chem. Soc. 28 (2) (2024) 101805, https://doi.org/10.1016/j.jscs.2023.101805.
[88] F. Al-Sheikh, F.T. Jasim, S.T. Al-Humairi, I. Hussein, A.A.J. Abdul Razak, Z. M. Shakor, S. Rohani, Adsorption of blue cationic thiazine dye from synthetic wastewater by natural Iraqi bentonite using response surface methodology: isotherm, kinetic, and thermodynamic studies, Chem. Afr. 6 (2023) 1437–1447, https://doi.org/10.1007/s42250-023-00591-w.
[89] K.M. Shabeeb, W.A. Noori, A.A. Abdulridha, H.S. Majdi, M.N. Al-Baiati, A. A. Yahya, K.T. Rashid, Z. Németh, K. Hernadi, Q.F. Alsalhy, Novel partially cross-linked nanoparticles graft co-polymer as pore former for polyethersulfone membranes for dyes removal, Heliyon 9 (11) (2023), https://doi.org/10.1016/j.heliyon.2023.e21958.
[90] W.A. Noori, A.A. Yahya, K.S. Alzubaidy, N.H. Jawad, R.A. Al-Juboori, K. T. Rashid, A.A. Abdulridha, M.N. Al-Baiati, S. Al-Saadi, Q.F. Alsalhy, Phthalic anhydride glycerol as a pore former for enhancing the surface and morphology of PVC ultrafiltration membrane, Desalin. Water Treat. 321 (2025) 101069, https://doi.org/10.1016/j.dwt.2025.101069.
[91] R.I. Raja, K.T. Rashid, M.A. Toma, Polyethersulfone/chamomile mixed matrix membrane for methylene blue dye removal from wastewater, Russ. J. Appl. Chem. 97 (1) (2024) 88–103, https://doi.org/10.1134/S1070427224010130.
[92] Y. Yahia, K.T. Rashid, M.A. Toma, K.S. Shakhir, T.M. Albayati, N.M.C. Saady, S. Zendehboudi, A novel green propolis (bee glue) nanoparticles mixed with Poly (Ether-Sulfone) ultrafiltration membrane for wastewater eriochrome Black T (EBT) and Congo red (CR) dye treatment, J. Environ. Chem. Eng. 13 (2) (2025) 115913, https://doi.org/10.1016/j.jece.2025.115913.
[93] M.Y. Ghadhban, K.T. Rashid, A.A. Abdulrazak, Q.F. Alsalhy, A novel poly (lactic-acid) and poly (butylene adipate-co-terephthalate) blend membrane modified with hesperidin for oily water emulsions separation, Chem. Eng. Res. Des. 206 (2024) 265–279, https://doi.org/10.1016/j.cherd.2024.05.020.
[94] M.Y. Ghadhban, K.T. Rashid, A.A. Abdulrazak, H. Meskher, Y. Benguerba, E.A. Y. Al-Sarraj, Q.F. Alsalhya, Optimal operational conditions of PLA/PBAT mixed matrix membrane for the treatment of oily wastewater, Eng. Technol. J. 42 (9 [Cheringmical Enginee]) (2024), https://doi.org/10.30684/etj.2024.150993.1774.
[95] S.H. Rasheed, S.S. Ibrahim, Q.F. Alsalhy, H.S. Majdi, Polydimethylsiloxane (PDMS) membrane for separation of soluble toluene by pervaporation process, Membranes (13) (2023) 289, https://doi.org/10.3390/membranes13030289.
[96] A.A. Abdul Aziz, M.A. Mokhter, A.I. Ghazali, N. Hanaffi, Removal of Remazol brilliant blue R dye from water using eggshell mixed matrix membrane through filtration and adsorption, J. Appl. Membr. Sci. Technol. 28 (3) (2024) 17–31, https://doi.org/10.11113/jamst.v28n3.302.
[97] N. Koutahzadeh, M.R. Esfahani, P.E. Arce, Sequential use of UV/H_2O_2—(PSF/TiO_2/MWCNT) Mixed matrix membranes for dye removal in water purification: membrane permeation, fouling, rejection, and decolorization, Env. Eng. Sci. 33 (6) (2016) 430–440, https://doi.org/10.1089/ees.2016.00.
[98] K. Parveen, U. Rafique, M.J. Akhtar, Fabrication of polysulfone mixed matrix membrane for wastewater treatment, J. Environ. Health Sci. Eng. 20 (2022) 757–774, https://doi.org/10.1007/s40201-022-00817-y.
[99] M. Manoukian, H. Fashandi, H. Tavakol, Polysulfone-highly uniform activated carbon sphere mixed-Matrix membrane intended for efficient purification of dye wastewater, Mater. Res. Express 6 (5) (2019), https://doi.org/10.1088/2053-1591/ab03fa.
[100] J. Zuo, M. Lu, J. Cai, R. Lan, X. Zeng, C. Zhou, Preparation of Am-MSN/PVDF mixed matrix membranes for enhanced removal of reactive black 5, Membranes 15 (2025) 42, https://doi.org/10.3390/membranes15020042.
[101] B. Baheri, R. Ghahremani, M. Peydayesh, M. Shahverdi, T. Mohammadi, Dye removal using 4A-zeolite/polyvinyl alcohol mixed matrix membrane adsorbents: preparation, characterization, adsorption, kinetics, and thermodynamics, Res. Chem. Intermed. 42 (6) (2015) 5309–5328, https://doi.org/10.1007/s11164-015-2362-1.
[102] M. Ghasemi Kochameshki, M. Mahmoudian, A. Marjani, Mixed-matrix membranes containing metal organic frameworks (MOFs) for separation of dyes and heavy metals from water, Arch. Hyg. Sci. 8 (1) (2019) 56–65, https://doi.org/10.29252/ArchHygSci.8.1.56.